



A Study on Novel Quantum Phenomena in Term of Impact Ionization

Neeru Kundu

Research Scholar, Department of Physics, Baba Mastnath University, Rohtak
(Neerukumarink21@gmail.com)

Abstract:

Since condensed-matter and materials are often thought to be well-defined and understood things (atoms) interacting with a well-defined and understood force, there are no fundamental intellectual difficulties remaining to find, actually, the opposite is true. Insulators have an energy gap for charge excitations, such that a collection of copper atoms with large interstices between them cannot conduct electricity. This is because the atoms are not strongly coupled to one another, hence their individual spectra are preserved. Solid copper is an efficient electrical conductor because its electrons "melt" into a new "liquid" phase when the atoms are compressed to absolute zero, even though this liquid phase has no excitation gap. Very little variations in atomic characteristics transform aluminium from a regular metal into a superconductor when the same experiment is carried out with aluminium atoms. The unexpected features of the large families of complex materials with many atoms per unit cell are still very difficult to anticipate a priori. In the next decade, this will be a crucial problem for theoretical researchers to solve.

Keywords: Aluminum, Atoms, Materials, Superconductor

Introduction:

Atomic energies generally fall on a range from 1 to 10 electron volts (eV). When analysing assemblages of atoms at progressively vast sizes, however, characteristic energies decline and excitations become more collective [1,2]. At low energies, effective elementary degrees of freedom may not be the same thing as individual electrons or atoms, and their interactions could seem quite different from the "bare" Coulomb ones. Some of the unexpected outcomes may be traced back to these snowball effects. In condensed-matter physics, we aim to grasp collective effects at ever-greater length scales [3, so this strategy is the exact opposite]. Like a particle accelerator, a refrigerator increases the inelastic collision distance and decreases the thermal energy scales across which particles collide. A sample in a dilution refrigerator is analogous to an extreme astrophysical system. Both fields share the conceptual challenge of providing convincing explanations of the physics that hold true over a wide range of scales. Fifty years ago, the development of the transistor was made possible by the discovery of a new quantum object called a hole. The discovery and understanding of many previously



unknown quantum events has made great strides in the last ten years. A short overview of many physical phenomena, such as superfluidity, superconductivity, Bose-Einstein condensation, quantum magnetism, and the quantum Hall effect [4]. Recent years have brought about significant progress in this final area, both technologically and theoretically. One application is the quantization of the conductance of electron "wave guides" in terms of e^2/h . A hole, a peculiar quantum phenomena whose expected existence was one of the first wins of quantum mechanics, was one of the most fascinating issues in condensed-matter physics around the time the transistor was conceived fifty years ago. The ability to create and regulate these "holes" is essential to the operation of electronic devices like as diodes, transistors, photocells, LEDs, solid-state lasers, and computer processors. Chemical dopants may be added to semiconductors to create either an electron surplus (n-type material) or a hole surplus (p-type material) [5].

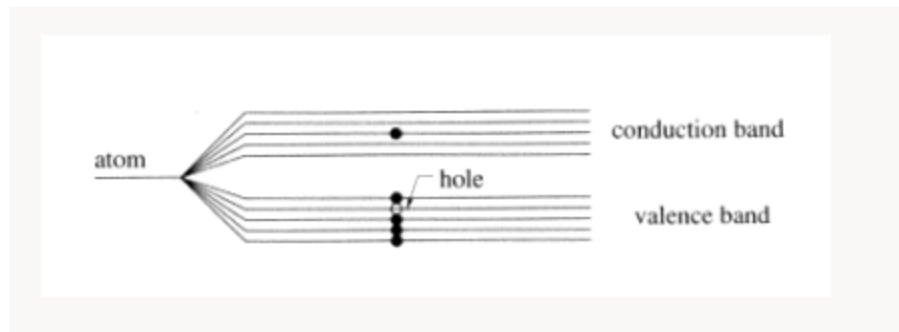


Figure 1: Energy bands in solids.

It is important to highlight the tight contact between experimentalists and theorists. Theorists in this discipline of physics are known to work closely with experimental groups, to the point that they routinely publish articles together. This tight cooperation, together with an exciting and constant stream of rather surprising experimental findings, is what gives the discipline its intellectual vigour.

Fundamental theoretical concepts like the Fermi liquid have been challenged by newly discovered electrical phenomena in complex and highly interacting materials. Totally novel ideas (such as fractionally charged quantum vortices) have been devised to elegantly describe the new phenomenology and expand the foundations of the field in situations like the fractional quantum Hall effect [6]. Paradoxes in high-temperature superconductivity and heavy-fermion systems have inspired several alternative paradigms, the viability of which is currently being debated. In order to meet this challenge, significant experimental and theoretical progress will be needed and made during the next decade.

Superconductivity and Superfluidity

Both superfluids and superconductors are unique in that they can transport matter or charge currents with zero resistance. Bose-Einstein condensation (discussed further below) causes helium-4 atoms to become superfluid at temperatures just above absolute zero. The effective

degree of freedom of electrons in a superconductor is very similar to that of a boson when they couple up. Cooper pairs of electrons in a typical low-temperature superconductor have a diameter that is substantially greater than the inter-electronic distance. Therefore, while the superconducting phase transition is analogous to Bose-Einstein condensation, the two concepts are not always interchangeable.

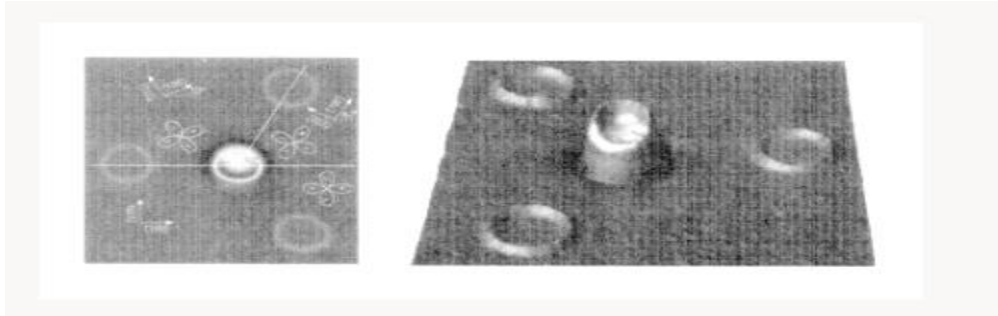


Figure 2: Strontium titanate films

Three strontium titanate films on a substrate, each with a distinct crystallographic orientation, are delineated by the long straight lines. All four of these concentric circles are genuinely epitaxially produced rings of the high-temperature superconductor yttrium barium copper oxide. The $d_{x^2-y^2}$ Cooper pair has a wave function that is perpendicular to the substrate and so points in the direction of the four-leaf clovers. A Josephson junction arises at the grain boundary as the ring crosses from one substrate to another. Cooper pairs that are moving from the lower right to the upper left are experiencing an orientation change of less than 45 degrees, thus their current and former states overlap positively. Tunneling in the reverse way, from the top down, is quite acceptable. Despite the fact that there is some overlap [7], the positive overlap is offset by the orientation change of more than 45 degrees from top right to bottom part. Due to the appearance of a unique vortex glass phase, it is obvious that H_{c2} , the upper critical field, is a totally mean-field idea. In mean-field theory, the sample is regarded "normal" when $H > H_{c2}$, but superconducting when $H < H_{c2}$. We can now see that H_{c2} is a crossover scale below which the order parameter rapidly increases to large values. Significant oscillations in high- T_c materials cause a vortex liquid zone where the resistivity is restricted despite the superconducting order parameter being massive [8]. Only when the system enters the frozen vortex glass phase can a true phase transition occur. When the vortices are permanently fixed in place, the dissipation stops.

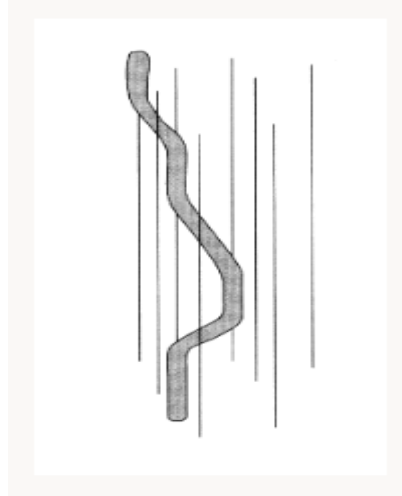


Figure 3: Superconductor vortex lines

The vortices seen in classical superconductors may be understood as the "world lines" of two-dimensionally moving quantum bosons in a single-dimensionally moving time-space. Tracing the boson paths across h/kBT is a requirement of the Feynman-man route integral model of quantum statistical mechanics. As a result, the "temperature" inversion of these phoney quantum bosons is dependent on the thickness of the superconducting sample. Bosons are exposed to a potential that is both spatially and temporally unpredictable thanks to the columnar flaws [8].

1130

Bose-Einstein Condensation in Atom Traps

For a long time, BECs were crucial in both high-energy and condensed-matter physics. It wasn't until 1938 [9] that BECs in superfluid helium were first seen. More recent experiments have shown physical evidence for the condensation of excitons in semiconductors. Hadronic elementary particle masses are also predicted to be generated via BEC. The unusual aspect of this parameter space is that of atomic vapours, which constitute a low-density domain in which the scattering length (the effective size of the particles) is substantially shorter than the typical particle spacing.

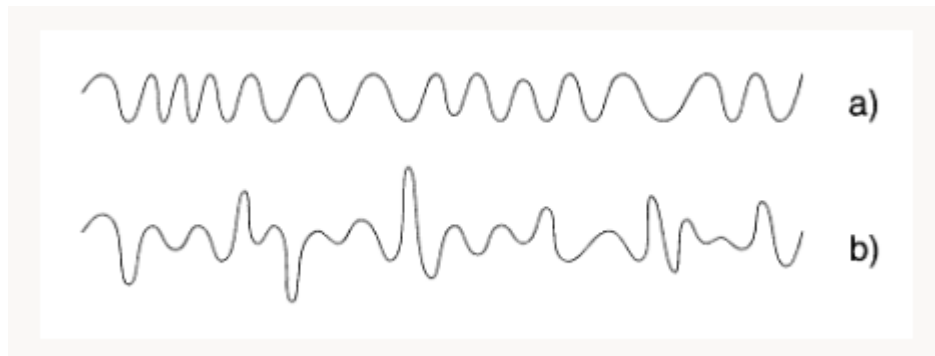


Figure 4: A laser produces coherent light

Coherent light, such as that generated by a laser, may be compared to a Bose condensate of photons. Bose-Einstein condensates (BECs) and atom lasers may be better understood if we grasp this concept. Consequently, we must examine variations to tell coherent light from incoherent light. In a condition of complete coherence, the expression " $\langle Y^\dagger Y^\dagger YY \rangle - \langle Y^\dagger Y \rangle^2 = 0$ ". According to the quantum mechanical interpretation, this means that the photons are not clumped together but rather follow a Poisson distribution. Extremely high intensity variations are produced by thermal sources because their fields are Gaussian random variables, and because Wick's theorem states that $\langle Y Y YY \rangle = 2! \langle Y Y \rangle^2$. According to the quantum interpretation, this extra "noise" or "bunching" is caused by fluctuations in the photon distribution. The chance of locating two bosons at the same location at the same time provides the potential energy of short-range interacting bosons in the atom trap [10]. We found, as predicted, that $\langle V \rangle_{\text{normal}} / \langle V \rangle_{\text{condensed}} = 2!$ in experiments comparing the normal and condensed states at the same density. The atomic vapour is so unstable that it spontaneously disintegrates into free-falling paired atoms. The decay rate is normal/YYY because a third body is required to remove the binding energy. The formula is 3! for compression. This third-order coherence effect has been experimentally seen, which is remarkable in and of itself.

Quantum Spin Chains and Ladders

Since the turn of the century, scientists have shown increased interest in quantum magnetism due to the synthesis of novel families of organic and inorganic compounds with spin-1/2 and spin-1 degrees of freedom. The discovery of high-temperature superconductors has led to significant advances in the synthesis of oxide compounds with spins arranged in two-dimensional planes, one-dimensional chains, quasi-one-dimensional ladders with both even and odd numbers of legs, and even two-dimensional arrays of intersecting one-dimensional chains. These novel systems have intriguing features and provide a great laboratory for testing ideas of highly coupled electronic systems [11]. The highest quantum-mechanical spin length, spin-1/2, was previously unavailable for investigation outside of very complex organometallic compounds. Since there is only a small coupling between the spins, any intriguing quantum effects in such materials only manifest at very low temperatures.

There is nothing like a quantum spin. "If its component in any direction is measured, it will always take on one of the discrete set of just $2S + 1$ values: $-S, -S + 1, \dots, S - 1, S$. This discreteness hints to substantial differences across quantum magnets, such as an excitation gap or other features that are sensitive to the precise value of S " [12]. Simultaneously, however, quantum mechanics possesses a different unique property that contradicts this discreteness. According to the laws of quantum physics, it is impossible to know for sure which state a spin is in [12]. "Linear superpositions of the $2S + 1$ discrete" basis states give rise to a continuous space of "coherent states." Because of this range of outcomes, the quantum spin may display some classical behaviour. A spin-1/2 may be set in any arbitrary transverse orientation, such as an up-



and-down linear combination. Very interesting physics emerges in quantum magnets as a result of this struggle between discrete and continuous models, which is similar to the more common wave-particle duality in quantum mechanics.

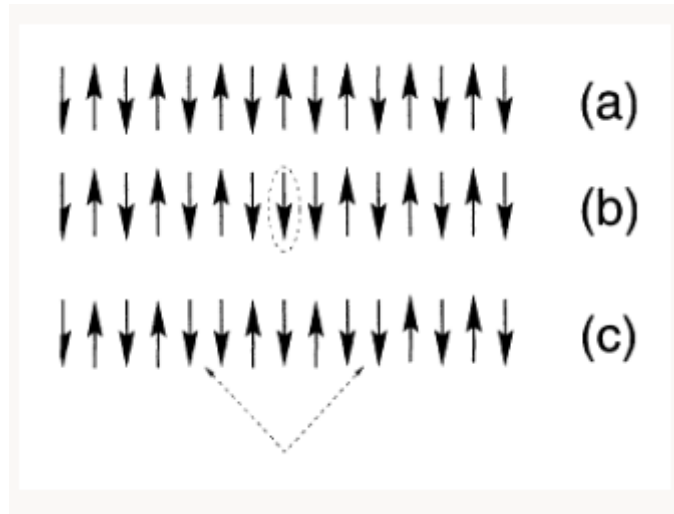


Figure 5: Illustration of the fractionalization procedure

Figure 5 is a graphical representation of the fractionalization procedure. Spins are perfectly aligned and antiferromagnetically organised in the first row. By inducing a single spin flip in the centre of the second row, an additional angular momentum of $S = 1$ has been added to the array. To preserve angular momentum, the third row depicts the time-evolved state achieved by a mutual spin flip of the two spins to the left and right of the centre spin. Now we can see that the initially reversed spin has split into two "domain walls" that are free to grow apart endlessly due to the fact that the space in between them is still properly organised in an antiferromagnetic fashion. Each of these domain-wall defects can be shown to behave, which is $S = 1$, according to the literature [12].

Spin-wave fractionalization opens up a lot of phase space for spin excitations, which has obvious experimental ramifications. The energy associated with each momentum in a normal spin wave is quantifiable. However, for a given overall momentum, a pair of spinons may have many distinct individual momentum states. This means that for a given momentum, there is a range of energies rather than a single energy (see Figure 6). Mutatis mutandis, the image we just painted for one-dimensional spin-1/2 chains also holds true for "odd-half-integer spins (1/2, 3/2, 5/2, etc.)"[13].



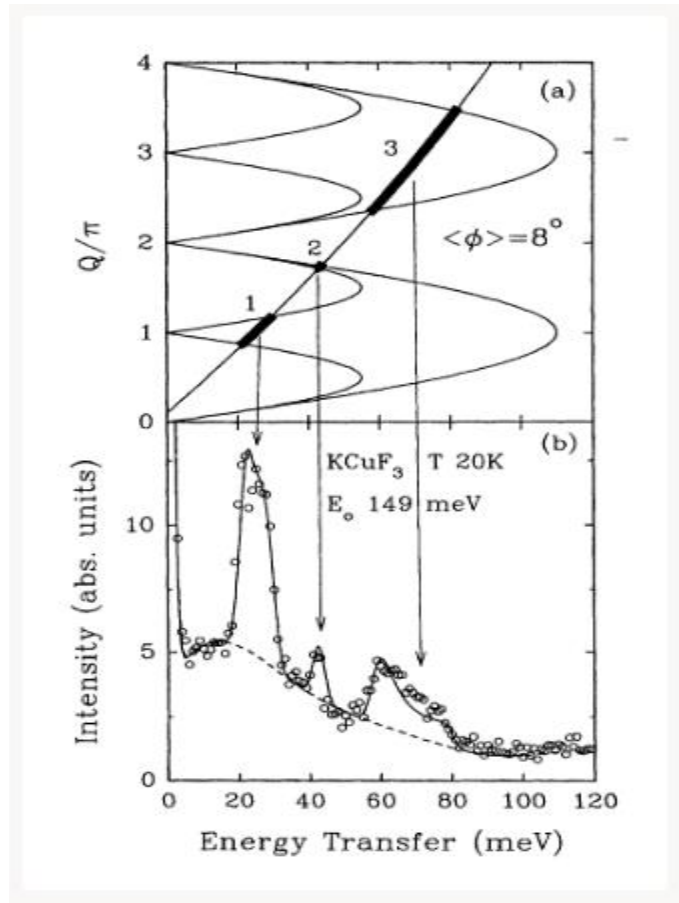


Figure 6: one-dimensional spin-1/2 chains

This case of spinon production was discovered by means of spin-flip inelastic neutron scattering. Compared to regular spin waves, the phase space available to spinons is far larger. The single spinon dispersion curve is shown as a periodic curve with period p in the upper panel. An upper bound on the allowed energy range for a pair of spinons with total momentum Q may be seen in the larger amplitude, period $2p$ curve. The maximum permitted momentum and energy transfer to the scattered neutrons is shown as a parabolic curve in the upper panel. Large peaks in the cross section are seen at energies predicted by the model in which a single flipped spin decays into two distinct spinon excitations (seen in the bottom panel). In accordance with standard spin wave theory, the first and third peaks should have no noticeable strength.

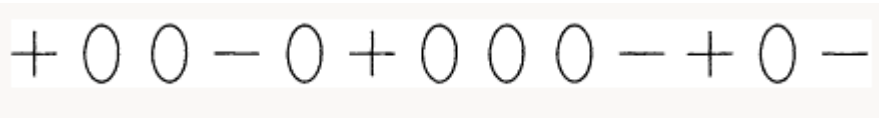


Figure 7: The spins in the ground state of the AKLT model

An alternative graphical representation of the AKLT ground also helps to explain the phenomenon that causes the excitation gap. One may think of the two spin-1/2 particles that



make up a $S = 1$ spin on a site. Singlet bonds between these spins and its surrounding spins form the "valence bond solid" shown. Spins on a site can only form a triplet and accurately represent $S = 1$ if the condition that the state is symmetric when two spins at a site are swapped (see Figure 8).

A single spin flip with $DS = 1$ may be split into two spinon excitations, one of which will have $S = 1/2$, much like the spin-1/2 chain. This phenomena is shown graphically in Figure 3.7b. To avoid the formation of additional unpaired spins, it has been discovered that a "string" of alternating double bonds and missing bonds [14] connects the two sites with the unpaired $S = 1/2$ spins. The "string tension" is the energy used in its formation, and it grows in direct proportion to the string's length. Thus, in contrast to the $S = 1/2$ chains, the spinons are confined (much like quarks), and the resulting excitation ("meson") has a finite minimum energy cost. The aforementioned topological order is shown to be broken by this excitation.

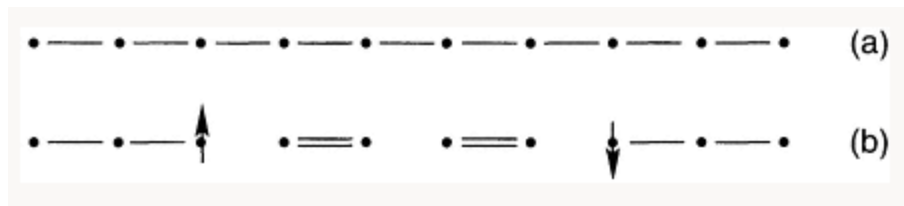


Figure 8: The condition in which the state is symmetric

Theoretical progress has been made toward a better understanding of the impact of "disorder in $S = 1/2$ and $S = 1$ one-dimensional quantum spin chains. When the $S = 1/2$ system transitions to a random singlet phase, connections between nearby particles are very strong, while those farther apart are arbitrarily weak"[14]. To the contrary, the $S = 1$ chain is initially gapped, making it resistant to low-level disorder. There is no longer a gap when there is a lot of disorder present, but the topological order remains in its Griffiths form [15]. Paradoxically, spins that disappeared at low energies in the pure system may be restored by injecting significant nonmagnetic impurity disturbance. An example of this notion is shown in Figure 9 for a segment of a " $S = 1$ chain that has been cut off from the rest of the chain by a nonmagnetic impurity at both ends. The valence bonds have been broken in the ground state of the solid, allowing for essentially free spin-1/2 at both ends of the segmen" [16]t. It is shown experimentally in the form of the magnetic susceptibility, which, at very low temperatures, adopts an algebraic rather than an exponential form.



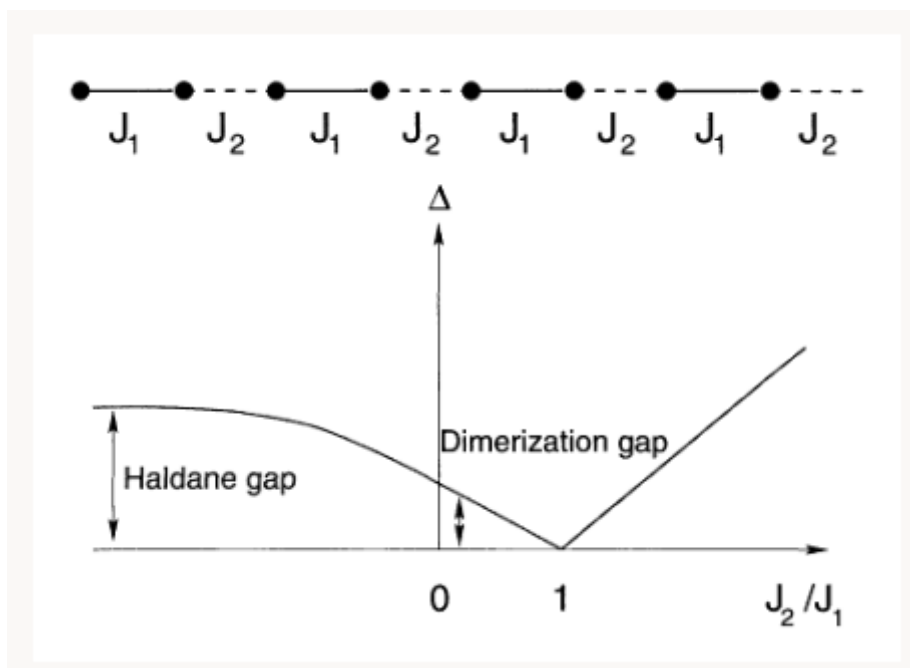


Figure 9: Nonmagnetic impurity links in the chain

The gap seen in dimerized systems is related to the gap observed in “ $S = 1$ (and other integer) chains. Think about the $S = 1/2$ chain”, which alternates between weak and strong links. For $J_2=0$, the precise ground state is a “valence bond solid” (VBS) of singlets on the J_1 bonds. Bond fluctuations occur at nonzero J_2 , however the gap persists in this area and the VBS state still describes the underlying physics. Even when the weak bond strength goes to zero and then changes sign to become ferromagnetic, the gap remains. The corresponding pairs of spins are locked into triplet states as these bonds become indefinitely ferromagnetic, and the $S = 1$ spin chain description is recovered. No phase transition occurs while the dimerization is tinkered with adiabatically because the gap remains open throughout. So, the “string” correlation function measures the same sort of topological order in the dimer system as it does in the “ $S = 1$ system, and the Haldane gap in the $S = 1$ system is a particular limit of the dimerization gap in the $S = 1/2$ system” [16].

Conclusion:

In terms of intellectual significance, the numerous quantum Hall effects are on par with superconductivity and superfluidity, two other amazing many-body phenomena discovered in the second half of the twentieth century. They constitute a very diverse array of events with profound and genuinely basic theoretical consequences. It is only in condensed-matter physics that an experimentalist may manually adjust the Chern-Simons angle or the number of flavours of relativistic chiral fermions. Some of the ideas from our earlier discussion of quantum spin chains pop up again. A gapped-charge liquid, with its own innovative type of hidden topological order, takes the place of the gapped-spin liquid previously described. Fractionalization of

quantum numbers and confinement/deconfinement of quasiparticle excitations are also brought up again.

References:

1. X. Li and J. Yang, "First-principles design of spintronics materials," *Natl. Sci. Rev.* 3, 365–381 (2016). <https://doi.org/10.1093/nsr/nww026>
2. M. C. Prestegard, G. P. Siegel, and A. Tiwari, "Oxides for spintronics: A review of engineered materials for spin injection," *Adv. Mater. Lett.* 5, 242–247 (2014). <https://doi.org/10.5185/amlett.2014.amwc1032>.
3. P. Liu, M. Wang, J. Ren, J. Liu, M. Xu, X. Huang, Z. Yu, and T. Zhou, "First-principle study on electronic structure and magnetism in doped MgO materials," *J. Supercond. Nov. Magn.* 35, 2037–2045 (2022). <https://doi.org/10.1007/s10948-022-06216-6>
4. M. Wang, T. Feng, J. Ren, L. Gao, H. Li, Z. Hao, Y. Yue, T. Zhou, and D. Hou, "First-principles study of the electronic structure and magnetism of the element-doped SnO₂ (001) surface," *J. Phys. Chem. Solids* 163, 110586 (2022).
5. M. Wang, M. Feng, and X. Zuo, "First principles study of the electronic structure and magnetism of oxygen-deficient anatase TiO₂ (001) surface," *Appl. Surf. Sci.* 292, 475–479 (2014). <https://doi.org/10.1016/j.apsusc.2013.11.165>
6. M. Wang, "First principle study of d^0 ferromagnetism in low-dimensional system," Doctoral dissertation (Nankai, University, 2014).
7. F. Goumrhar, L. Bahmad, O. Mounkachi, and A. Benyoussef, "Ab initio calculations of the magnetic properties of TM (Ti, V)-doped zinc-blende ZnO," *Int. J. Mod. Phys. B* 31, 1850025 (2017). <https://doi.org/10.1142/S021797921850025X>.
8. S. Ostanin, A. Ernst, L. M. Sandratskii, P. Bruno, M. Däne, I. D. Hughes, J. B. Staunton, W. Hergert, I. Mertig, and J. Kudrnovský, "Mn-stabilized zirconia: From imitation diamonds to a new potential high- T_c ferromagnetic spintronics material," *Phys. Rev. Lett.* 98, 016101 (2007). <https://doi.org/10.1103/PhysRevLett.98.016101>.
9. S. M. Woodley, S. Hamad, J. A. Mejías, and C. R. A. Catlow, "Properties of small TiO₂, ZrO₂ and HfO₂ nanoparticles," *J. Mater. Chem.* 16, 6203–6231 (2006). <https://doi.org/10.1039/b600662k>.
10. A. Lamperti, E. Cianci, R. Ciprian, L. Capasso, E. Weschke, and A. Debernardi, "Magnetic properties of iron doped zirconia as a function of Fe concentration: From ab initio simulations to the growth of thin films by atomic layer deposition and their characterization by synchrotron radiation," *J. Vac. Sci. Technol. A* 36, 02D404 (2018). <https://doi.org/10.1116/1.5016028>.
11. H. Römer, K.-D. Luther, and W. Assmus, "Measurement of the distribution coefficient of neodymium in cubic ZrO₂," *J. Cryst. Growth* 130, 233–237 (1993). [https://doi.org/10.1016/0022-0248\(93\)90856-R](https://doi.org/10.1016/0022-0248(93)90856-R).



12. F. Goumrhar, L. Bahmad, O. Mounkachi, and A. Benyoussef, "Magnetic properties of vanadium doped CdTe: Ab-initio calculations," J. Magn. Magn. Mater. 428, 368–371 (2017). <https://doi.org/10.1016/j.jmmm.2016.12.041>.
13. A. Ait Raiss, Y. Sbai, L. Bahmad, and A. Benyoussef, "Magnetic and magneto-optical properties of doped and co-doped CdTe with (Mn, Fe): Ab-initio study," J. Magn. Magn. Mater. 385, 295–301 (2015). <https://doi.org/10.1016/j.jmmm.2015.02.077>.
14. F. Goumrhar, L. Bahmad, O. Mounkachi, and A. Benyoussef, "Ab-initio calculations for the electronic and magnetic properties of Cr doped ZnTe," Comput. Condens. Matter 15, 15–20 (2018). <https://doi.org/10.1016/j.cocom.2018.03.003>.
15. M. Wang, L. Gao, J. Ren, D. Hou, Y. Yue, and T. Zhou, "Ab initio study on magnetism of SnO₂ (110) surface with non-metallic elements doping," Mater. Sci. Semicond. Process. 137, 106194 (2022). <https://doi.org/10.1016/j.mssp.2021.106194>.
16. M. Zhou, Y. Zhang, L. Sun, W. Hao, E. Cao, and Z. Yang, "Influence of oxygen adsorption for vacancy-induced d^0 magnetism in rutile TiO₂ (001) surface," Appl. Surf. Sci. 492, 135–142 (2019). <https://doi.org/10.1016/j.apsusc.2019.06.206>.
17. Y. Ziat, M. Boujnah, A. Benyoussef, and A. El Kenz, "Magnetic properties of Co-(Os, Mn) Co-doped ZrO₂ within GGA and mBJ approaches," J. Supercond. Nov. Magn. 28, 3397–3403 (2015). <https://doi.org/10.1007/s10948-015-3171-x>.
18. Y. Xie, A.-N. Zhou, Y.-T. Zhang, Y.-P. Huo, S.-F. Wang, and J.-M. Zhang, "First principles study of structural, magnetic and electronic properties of N-doped monoclinic ZrO₂," J. Magn. Magn. Mater. 387, 58–61 (2015).
19. M. Boujnah, H. Labrim, K. Allam, A. Belhaj, A. Benyoussef, A. El Kenz, B. Belhorma, and A. El Bouari, "Magnetic and electronic properties of point defects in ZrO₂," J. Supercond. Nov. Magn. 26, 2429–2434 (2013). <https://doi.org/10.1007/s10948-012-1826-4>.
20. F. Goumrhar, L. Bahmad, O. Mounkachi, and A. Benyoussef, "Ferromagnetism in Mn and Fe doped ZrO₂ by ab-initio calculations," Comput. Condens. Matter 19, e00361 (2019). <https://doi.org/10.1016/j.cocom.2018.e00361>.

